

Stray fields based magnetoresistance mechanism in Ni₈₀Fe₂₀-Nb-Ni₈₀Fe₂₀ trilayers

D. Stamopoulos,* E. Manios, and M. Pissas

Institute of Materials Science, NCSR "Demokritos", 153-10, Aghia Paraskevi, Athens, Greece.

(Dated: February 1, 2008)

In this work we report on the transport and magnetic properties of hybrid trilayers (TLs) and bilayers (BLs) that consist of low spin polarized Ni₈₀Fe₂₀ exhibiting in-plane but no uniaxial anisotropy and low-T_c Nb. We reveal a magnetoresistance effect of magnitude identical to the one's that were reported in [V. Peña et al., Phys. Rev. Lett. **94**, 57002 (2005)] for TLs consisting of highly spin polarized La_{0.7}Ca_{0.3}MnO₃ and high-T_c YBa₂Cu₃O₇. The presented effect is pronounced when compared to the one reported in [A.Yu. Rusanov et al., Phys. Rev. B **73**, 060505(R) (2006)] for Ni₈₀Fe₂₀-Nb-Ni₈₀Fe₂₀ TLs of strong in-plane uniaxial anisotropy. In our TLs the magnetoresistance exhibits an increase of two orders of magnitude when the superconducting state is reached: from the conventional normal-state values $\Delta R/R_{nor} \times 100\% = 0.6\%$ it goes up to $\Delta R/R_{nor} \times 100\% = 45\%$ ($\Delta R/R_{min} \times 100\% = 1000\%$) for temperatures below T_c^{SC}. In contrast, in the BLs the effect is only minor since from $\Delta R/R_{nor} \times 100\% = 3\%$ in the normal state increases only to $\Delta R/R_{nor} \times 100\% = 8\%$ ($\Delta R/R_{min} \times 100\% = 70\%$) for temperatures below T_c^{SC}. Magnetization data of both the *longitudinal* and *transverse* magnetic components are presented. Most importantly, in this work we present data not only for the normal state of Nb but also in its superconducting state. Strikingly, these data show that *below its T_c^{SC} the Nb interlayer under the influence of the outer Ni₈₀Fe₂₀ layers attains a magnetization component transverse to the external field*. By comparing the transport and magnetization data we propose a new candidate mechanism that could motivate the pronounced magnetoresistance effect observed in the TLs. Adequate magnetostatic coupling of the outer Ni₈₀Fe₂₀ layers is motivated by stray fields that emerge naturally in their whole surface due to the multidomain magnetic structure that they attain near coercivity. Consequently, the stray fields penetrate the Nb interlayer and suppress its superconducting properties by primarily (secondarily) exceeding its lower (upper) critical field. Atomic force microscopy is employed in order to examine the possibility that such magnetostatic coupling could be promoted by interface roughness. Referring to the BLs, although out-of-plane rotation of the single Ni₈₀Fe₂₀ layer is still observed, in these structures magnetostatic coupling doesn't occur due to the absence of a second Ni₈₀Fe₂₀ one so that the observed magnetoresistance peaks are only modest.

PACS numbers: 74.45.+c, 74.78.Fk, 74.78.Db

I. INTRODUCTION

Recently, superconducting-ferromagnetic (SC-FM) hybrids have attracted much interest due to the general expectation that both interesting features and subsequent application devices could emerge owing to the deliberate mixing of these two long-range phenomena.^{1,2,3,4,5,6,7,8,9,10,11,12,13} A very representative elemental apparatus is the superconducting spin valve that was theoretically proposed in Refs.14,15. It is based on a FM-SC-FM trilayer (TL) where, as it was proposed^{14,15} the nucleation of superconductivity can be controlled by the *relative* magnetization orientation of the outer FM layers. J.Y. Gu et al.¹ were the first who reported on the experimental realization of a [Ni₈₂Fe₁₈-Cu_{0.47}Ni_{0.53}]/Nb/[Cu_{0.47}Ni_{0.53}-Ni₈₂Fe₁₈] spin valve. I.C. Moraru et al.² also studied a great number of Ni-Nb-Ni TLs and observed a significantly larger shift of the superconducting transition temperature T_c^{SC} than that reported in Ref.1. In these works^{1,2} the exchange bias was employed in order to "pin" the magnetization of the one FM layer and it was observed that when the magnetizations of the two FM layers were parallel (antiparallel) the resistive transition of the SC was placed at lower (higher) temperatures. V. Peña et al.³ and A.Yu.

Rusanov et al.⁴, studied La_{0.7}Ca_{0.3}MnO₃-YBa₂Cu₃O₇-La_{0.7}Ca_{0.3}MnO₃ and Ni₈₀Fe₂₀-Nb-Ni₈₀Fe₂₀ TLs, respectively. In agreement to what we have also reported in our recent work⁹ both studies^{3,4} reported that the antiparallel magnetization configuration of the FM layers suppresses superconductivity when compared to the parallel case. Interestingly, in the work of Peña et al.³ a magnetoresistance effect of the order 1000% was observed in the TLs that it was related to the occurrence of spin imbalance¹⁶ in the SC ultimately motivated by the high spin polarization (almost 100%) of La_{0.7}Ca_{0.3}MnO₃.

An alternative underlying mechanism is proposed in the present work for the interpretation of a similar effect having identical magnitude for the case of TLs constructed by two completely different FM and SC ingredients: low spin polarized Ni₈₀Fe₂₀ and low-T_c Nb. We note that the Ni₈₀Fe₂₀ layers employed in this work were deposited at *room temperature* with *no* magnetic field applied during the deposition (see the preparation details below). They exhibit strong in-plane but no uniaxial anisotropy. We observed that for T < T_c^{SC} the Ni₈₀Fe₂₀-Nb-Ni₈₀Fe₂₀ TLs exhibit an extreme zero-field increase of the measured MR which amounts to $\Delta R/R_{nor} \times 100\% = 45\%$ ($\Delta R/R_{min} \times 100\% = 1000\%$). Beside the TLs more simple Nb-Ni₈₀Fe₂₀ bilayers (BLs) have also been studied. In these BLs the effect under discussion is mini-

mum since it amounts to only $\Delta R/R_{nor} \times 100\% = 8\%$ ($\Delta R/R_{min} \times 100\% = 70\%$). In the normal state of the SC interlayer both TLs and BLs present conventional magnetoresistance which by no means exceeds 0.6% and 3%, respectively.

Magnetization measurements of both the *longitudinal* and *transverse* magnetic components (in respect to the external magnetic field) revealed that the TL exhibits almost completely reversible longitudinal magnetization with nearly zero remanence, while its respective transverse component attains significant values near zero field indicating a magnetostatic coupling of the outer $\text{Ni}_{80}\text{Fe}_{20}$ layers. *Most importantly, these results clearly show that below its T_c^{SC} the Nb interlayer attains a magnetization component transverse to the external magnetic field under the influence of the outer $\text{Ni}_{80}\text{Fe}_{20}$ layers.* These magnetic characteristics indicate that in our samples the magnetoresistance effect is motivated by a transverse magnetization component related to the stray fields that near coercivity emerge naturally in the whole surface of the outer $\text{Ni}_{80}\text{Fe}_{20}$ layers due to the multidomain magnetic structure that they attain. As these stray fields interconnect the outer $\text{Ni}_{80}\text{Fe}_{20}$ layers through the Nb interlayer they surely exceed its lower or even *locally* amount to its upper critical field. Accordingly, current induced vortex motion (if only the SC's lower critical field is exceeded) or *localized* normal state areas (if even the SC's upper critical field is *locally* overstepped) could motivate the observed dissipation, respectively. Since it is well known that interface roughness could promote stray-fields induced magnetostatic coupling in relevant layered structures^{17,18,19,20} we also use atomic force microscopy (AFM) in order to examine this possibility. Referring to the BLs although out-of-plane rotation of the single $\text{Ni}_{80}\text{Fe}_{20}$ layer is still observed, due to the absence of a second one in these structures magnetostatic coupling doesn't occur so that the observed magnetoresistance peaks are only modest.

Finally, a comparison with current experiments is made. Referring to the BLs we note that the smooth magnetoresistance effect that we observe in our Nb- $\text{Ni}_{80}\text{Fe}_{20}$ hybrids qualitatively resembles the one reported by V.V. Ryazanov et al. in Ref.21 for the case of Nb- $\text{Cu}_{0.43}\text{Ni}_{0.57}$ BLs. Regarding the TLs, the main mechanism that we propose for the interpretation of the intense peaks that are obtained in our $\text{Ni}_{80}\text{Fe}_{20}$ -Nb- $\text{Ni}_{80}\text{Fe}_{20}$ hybrids is different from the one proposed by V. Peña et al.³ and by A. Yu. Rusanov et al.⁴ for $\text{La}_{0.7}\text{Ca}_{0.3}\text{MnO}_3$ - $\text{YBa}_2\text{Cu}_3\text{O}_7$ - $\text{La}_{0.7}\text{Ca}_{0.3}\text{MnO}_3$ and $\text{Ni}_{80}\text{Fe}_{20}$ -Nb- $\text{Ni}_{80}\text{Fe}_{20}$ ones, respectively. Reasons responsible for the existing differences are discussed.

II. PREPARATION OF SAMPLES AND EXPERIMENTAL DETAILS

The samples were sputtered on Si [001] substrates under an Ar environment (99.999% pure). In order to

eliminate the residual oxygen that possibly existed in the chamber we performed Nb pre-sputtering for very long times.^{22,23} During the pre-sputtering process all the residual oxygen was absorbed by the dummy Nb since it acts as a strong oxygen getter. This procedure has a direct impact on the quality of the produced films.^{22,23} The Nb layers were deposited by dc-sputtering at 46 W and an Ar pressure of 3 mTorr, while for the $\text{Ni}_{80}\text{Fe}_{20}$ (NiFe) layers rf-sputtering was employed at 30 W and 4 mTorr. We should stress that: (i) all depositions were carried out *at room temperature* and (ii) *no* external magnetic field was applied hereon during the deposition of the NiFe layers. However, the samples can't be shielded from the residual magnetic fields existing in the chamber of our magnetically-assisted-sputtering unit. Measurements by means of a Hall sensor revealed that at the place where the substrates are mounted the residual fields exhibit parallel components of magnitude 10–15 Oe at maximum. Thus, our NiFe films exhibit in-plane anisotropy. However, they don't exhibit detectable uniaxial anisotropy since the magnetic field sources are placed symmetrically on the perimeter of the circular rf-gun. The produced films have low coercive fields of order 20 Oe. In this work we show detailed results for NiFe(19)-Nb(50)-NiFe(38) TLs and Nb(50)-NiFe(38) BLs (in nanometer units). Both qualitatively and quantitatively similar results were obtained in NiFe(19)-Nb(50)-NiFe(19) TLs and Nb(50)-NiFe(19) BLs.

Our magnetoresistance measurements were performed by applying a dc-transport current (always normal to the magnetic field) and measuring the voltage in the standard four-point straight configuration. In most of the measurements the applied current was $I_{dc} = 0.5$ mA, which corresponds to an effective density $J_{dc} \approx 1000$ A/cm² (typical in plane dimensions of the films are 6×5 mm²). The temperature control and the application of the magnetic fields were achieved in a superconducting quantum interference device (SQUID) (Quantum Design). In all cases the applied field was parallel to the films.

III. EXPERIMENTAL RESULTS

A. Magnetoresistance data

As may be seen in Fig. 1(a) the zero-field critical temperature is $T_c^{SC} = 7.42$ K and $T_c^{SC} = 7.6$ K for the TL and the BL, respectively. The slightly lower critical temperature of the TL is fairly justified since owing to the proximity effect the two outer NiFe layers of the TL suppress stronger the superconducting order parameter when compared to the BL. Figures 1(b) and 1(c) show the main raw experimental results of our work. Presented are detailed voltage curves $V(H)$ as a function of magnetic field for both the TL, panel (b) and the BL, panel (c) that were obtained in various temperatures across their zero-field resistive curves that are presented in panel (a). We clearly see that the TL exhibits a completely different

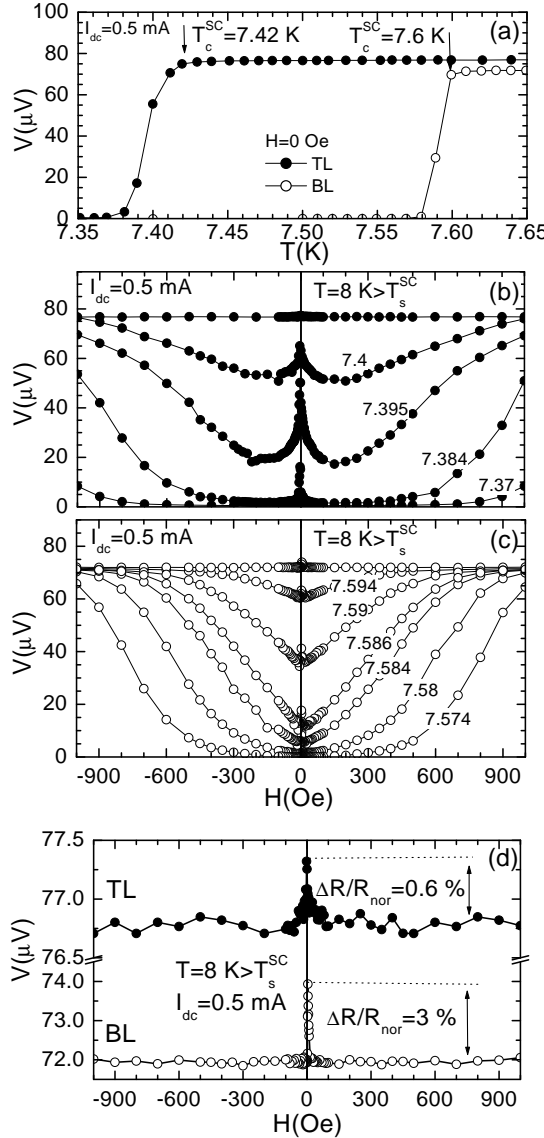


FIG. 1: (a) Zero-field resistive curves $V(T)$ of a TL (solid circles) and a BL (open circles), respectively. Detailed $V(H)$ curves for a TL (b) and for a BL (c) at various temperatures across their resistive transitions presented in (a). In panel (d) we focus on the respective curves observed in the normal state for both the TL (solid circles) and the BL (open circles).

behavior when compared to the BL. While as the magnetic field is lowered from 1000 Oe the resistance of both structures decreases, it is the resistance of the TL that below a threshold value increases strongly exhibiting a maximum at around zero field. The field's regime where the resistance increase is observed in the TL extends to no more than 300 – 400 Oe. In contrast, the respective curves of the BL present only a minor increase for 5 – 10 Oe around zero field.

The magnetoresistance effect observed in the TL is strong. The percentage resistance change $(R(0) - R(H))/R(H) \times 100\%$ meets the criteria for considered as

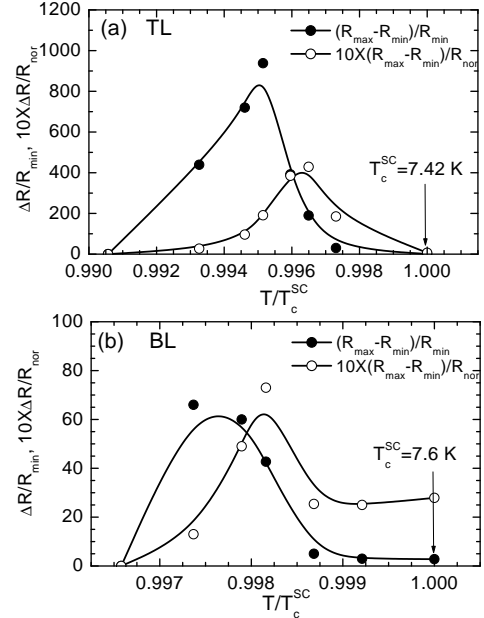


FIG. 2: Percentage change of the MR as calculated according to two definitions $(R_{max} - R_{min})/R_{min} \times 100\%$ and $(R_{max} - R_{min})/R_{nor} \times 100\%$ for the TL (a) and the BL (b). In both panels the data referring to the second definition $(R_{max} - R_{min})/R_{nor} \times 100\%$ are multiplied by a factor of 10 for the sake of presentation.

giant magnetoresistance. Figures 2(a) and 2(b) present the respective data for the TL and the BL as a function of the reduced temperature according to two definitions. The first one is $(R_{max} - R_{min})/R_{min} \times 100\%$ (solid circles) and takes into account the minimum (around 150 – 200 Oe) and maximum (around 0 Oe) values of the experimental curves. The second one, which is modest and surely more relevant for the study of the underlying physics, is $(R_{max} - R_{min})/R_{nor} \times 100\%$ (open circles) and takes into account the resistance that the SC exhibits in its normal state. In Fig. 2(a) we see that for the TL the maximum MR is obtained halfway the resistive transition of the SC, at $T/T_c^{SC} = 0.995$ and amounts to almost 1000% according to the first definition. But even according to the modest definition $(R_{max} - R_{min})/R_{nor} \times 100\%$ the observed increase amounts to 45% which is well inside the range of giant magnetoresistance (notice that for the sake of presentation in both panels these data are multiplied by a factor of 10). Figure 2(b) presents the respective data for the BL. In contrast to the TL, for the BL the maximum magnetoresistance is obtained near the bottom of its resistive transition, at $T/T_c^{SC} = 0.9973$ and doesn't exceed 70% (8%) according to the first (second) definition. *It is obvious that the effect observed in the TL is at least one order of magnitude stronger than the one of the BL.* Despite the differences discussed above we have to stress that in both structures the effect is not observed in the normal state of the SC. More specifically, for $T > T_c^{SC}$ conventional magnetoresistance is revealed with

values 0.6% and 3% for the TL and BL, respectively as it is presented in Fig.1(d).

B. Magnetization data

In order to investigate the underlying mechanism responsible for the magnetoresistance effect we performed detailed magnetization loop measurements both well below and above the superconducting transition of Nb. We found out that the $m(H)$ loop of the NiFe(19)-Nb(50)-NiFe(38) TL obtained at $T = 8 \text{ K} > T_c^{SC}$ is almost totally reversible and exhibits nearly zero remanent magnetization. Detailed results are presented in Figs.3(a) and 3(b) in an extended and in the low-field regime, respectively. This fact was surprising since we had previously observed that the respective loops of single NiFe layers exhibit clear irreversibility and coercivity in the range 10 – 20 Oe. Thus, we investigated this behavior further. Except for the $m(H)$ loop for the TL (denoted by triangles) we also present data for two different BLs: a NiFe(19)-Nb(50) (solid circles) and a Nb(50)/NiFe(38) (open circles). Notice that these two BLs are the main building blocks of the complete TL. We prepared the two BLs in order to examine if it was possible to reproduce the $m(H)$ loop of the TL by decomposing it into its two main parts. This would allow us to examine whether the two outer NiFe layers of the complete TL *do interact* or the total $m(H)$ loop is a simple superposition of the two basic $m(H)$ loops. We stress that we preferred to examine the two NiFe(19)-Nb(50) and Nb(50)-NiFe(38) BLs and not the two single NiFe(19) and NiFe(38) layers since we wanted to take into account any possible parameter that could influence the magnetic behavior of the NiFe layers. For instance, strain could be induced in each NiFe layer by the adjacent Nb layer due to the mismatch of their lattices so that the magnetic $m(H)$ loop of each FM layer could be altered even slightly. The obtained results are revealing. We clearly see that by adding appropriately the $m(H)$ loops of the two BLs we may reproduce the loop of the complete TL only in the high-field regime. The zeroing of both the coercive field and of remanent magnetization that is observed in the TL can't be reproduced. Thus, we may safely conclude that in the low field regime the two NiFe layers participating the TL strongly interact through the Nb interlayer so that the magnetic behavior of the complete TL resembles the one of a soft FM both above and below T_c^{SC} (see Figs.3(a)-3(b) and Fig.4(b), respectively). In contrast, for high magnetic fields the interaction between each NiFe layer with the external magnetic field dominates so that they practically become uncoupled.

A plausible mechanism that is compatible with the almost zeroing of the remanent magnetization that is observed only in the TLs is the antiparallel alignment of the two outer NiFe layers' magnetizations. However, owing to the specific conditions that were used during the deposition it is unnatural to assume that our samples ex-

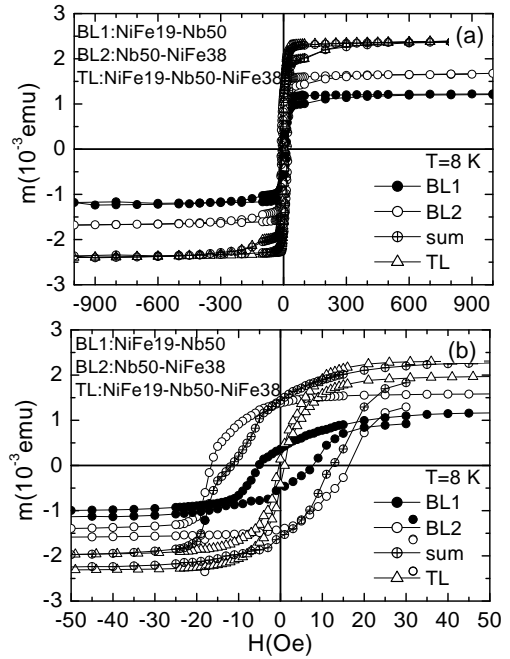


FIG. 3: Magnetization loop data obtained at $T = 8 \text{ K} > T_c^{SC}$ for the NiFe(19)-Nb(50)-NiFe(38) TL (triangles), a NiFe(19)-Nb(50) BL1 (solid circles) and a Nb(50)-NiFe(38) BL2 (open circles). Circles with crosses correspond to the simple addition of the $m(H)$ loops of the BL1 and BL2 (see text for details). All data are presented in an extended field regime (a) and for low magnetic fields (b). In these measurements the magnetic field was parallel to the sample in all cases.

hibit a *coherent* magnetization reversal with antiparallel relative configuration in the low field regime as it was observed in Refs.3,4. In addition, the Nb interlayer is *thick* so that it can't probably maintain an exchange coupling of the outer NiFe layers. Thus, a complete antiferromagnetic exchange coupling of the outer NiFe layers as this occurs in usual giant magnetoresistance spin valves of *thin* normal metal interlayer^{24,25,26} can't be achieved in our case. Accordingly, other mechanisms should be investigated. Since the data presented in Fig.3 refer to the longitudinal component of the TL's magnetization (in respect to the external magnetic field) they don't provide any information on its transverse component. This information is quite important since the zeroing of the TL's remanent (longitudinal) magnetization could not be exclusively related to either an antiparallel alignment of the outer NiFe layers but could be motivated by the fact that the magnetization rotates out-of-plane so that it becomes transverse and can't be detected by the longitudinal set of pick-up coils in our SQUID. Thus, we performed additional measurements focused on the transverse magnetic component.

Representative results obtained above and well below T_c^{SC} are shown in Figs.4(a)-4(b) for a TL. Presented are both the longitudinal (solid circles) and transverse (open

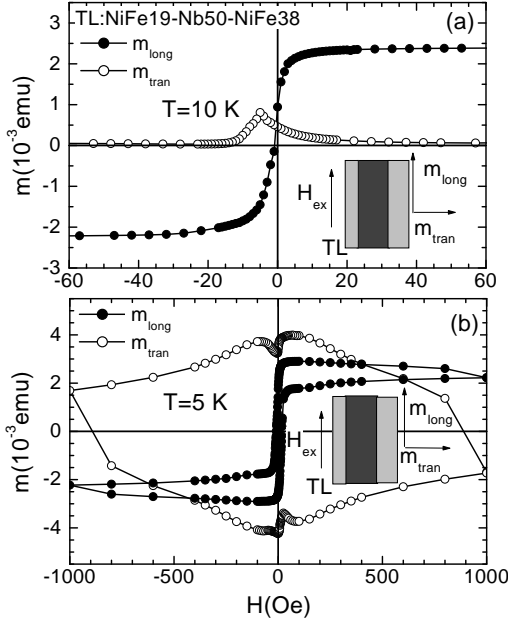


FIG. 4: Magnetization data obtained in a NiFe(19)-Nb(50)-NiFe(38) TL (a) at $T = 10 \text{ K} > T_c^{SC}$ and (b) at $T = 5 \text{ K} < T_c^{SC}$ for both the longitudinal (solid circles) and transverse (open circles) components. The inset in each panel presents schematically in side view the configuration of the external field and of each magnetic component of the TL. In these measurements the external field was parallel to the TL.

circles) components. We stress that magnetization data for the superconducting regime, and most importantly for the transverse magnetic component, are presented for the first time.^{1,2,3,4,9} The insets present the configuration of the external field and of each magnetic component. Let us first discuss panel (a), that is the normal state data obtained at $T = 10 \text{ K} > T_c^{SC}$ while the applied field is lowered from positive saturation. We clearly see that as the external field passes through zero the transverse magnetic component of the TL attains significant values of the order 40% of the saturated longitudinal one. This clearly proves that in our samples a significant part of the TL's magnetization rotates out-of-plane near zero magnetic field. Proceeding with the data of panel (b), that were obtained in the superconducting state at $T = 5 \text{ K} < T_c^{SC}$ we stress that these data reveal a surprising feature: the out-of-plane rotation of the TL's magnetization is not observed only in the normal state but also well inside the superconducting state of Nb. We see that even at $T = 5 \text{ K}$ the longitudinal component resembles the loop of a FM as if the SC was absent (the only fingerprint of its presence comes from the comparatively small irreversibility that shows up). More importantly, we see that it is the transverse component of the TL that obtains the model loop expected for a SC. *These results clearly prove that the SC behaves diamagnetically not in respect to the parallel external field but in respect to a new transverse field that emerges owing to the magnetic coupling of the*

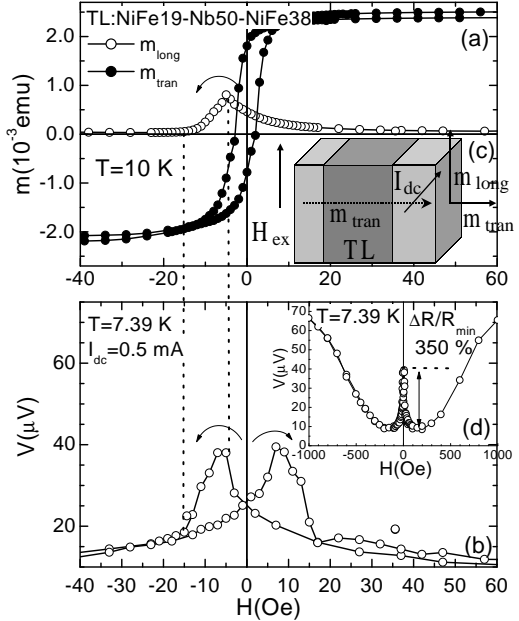


FIG. 5: (a) Both branches of the longitudinal (solid circles) and decreasing branch of the transverse (open circles) magnetic components obtained at $T = 10 \text{ K} > T_c^{SC}$ and (b) both branches of the magnetoresistance curve obtained at $T = 7.39 \text{ K} < T_c^{SC}$ for a NiFe(19)-Nb(50)-NiFe(38) TL. Inset (c) presents schematically the configuration for both the magnetization and transport measurements, while inset (d) shows the magnetoresistance curve in an extended field range. In these measurements the external field was parallel to the TL.

outer NiFe layers.

C. Comparison of low field data

The results that were presented above indicate that probably the out-of-plane rotation of the TL's magnetization is related to the observed magnetoresistance peaks. To investigate this possibility thoroughly in Figs.5(a) and 5(b) we compare detailed measurements of the longitudinal (solid circles) and the transverse (open circles) magnetic components (obtained at $T = 10 \text{ K} > T_c^{SC}$) and of the magnetoresistance (obtained at $T = 7.39 \text{ K} < T_c^{SC}$), respectively. These data are focused at low magnetic fields. Inset (c) shows schematically the configuration for both the magnetization and transport measurements, while inset (d) shows the magnetoresistance curve in an extended field range. We clearly see that *the maximum of the TL's transverse component coincides with the magnetoresistance peak*. In addition, the zeroing of the transverse magnetization is accompanied by an abrupt change in the slope of the $V(H)$ curve. *This experimental fact indicates that in the TLs the out-of-plane rotation of the magnetization is probably responsible for the observed magnetoresistance peaks.*

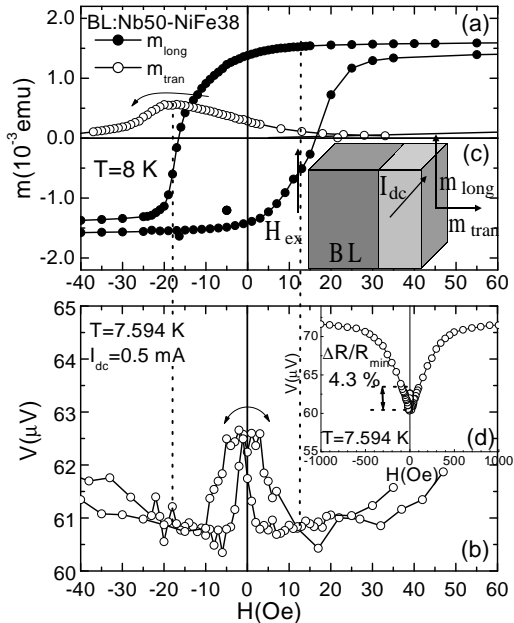


FIG. 6: (a) Both branches of the longitudinal (solid circles) and decreasing branch of the transverse (open circles) magnetic components obtained at $T = 10 \text{ K} > T_c^{SC}$ and (b) both branches of the magnetoresistance curve obtained at $T = 7.594 \text{ K} < T_c^{SC}$ for a Nb(50)-NiFe(38) BL. Inset (c) presents schematically the configuration of both the magnetization and the transport measurements, while inset (d) shows the magnetoresistance curve in an extended field range. In these measurements the external field was parallel to the BL.

To investigate if this holds also for the case of BLs we performed the respective measurements in the low field regime. Representative results of the longitudinal (solid circles) and transverse (open circles) magnetic components (obtained at $T = 8 \text{ K} > T_c^{SC}$) and of the magnetoresistance (obtained at $T = 7.594 \text{ K} < T_c^{SC}$) are shown in Figs.6(a) and 6(b), respectively. Inset (c) shows schematically the configuration for both the magnetization and transport measurements, while inset (d) shows the magnetoresistance curve in an extended field range. The direct comparison reveals that the maximum of the BL's transverse component follows the zeroing of the longitudinal one. More importantly, we see that *in the BLs the minor magnetoresistance peak is clearly not related to the out-of-plane rotation of the magnetization since it is placed at almost zero magnetic field*.

IV. DISCUSSION

Summarizing the data presented so far we conclude that: (i) The magnetoresistance effect observed in the TLs is one order of magnitude stronger than the one of the BLs (see Figs.2(a)-2(b)). (ii) When the NiFe layers are brought together through a Nb interlayer they strongly interact so that almost zeroing of both the lon-

gitudinal remanent magnetization and coercivity is observed (see Fig.3). In contrast, the height of the transverse magnetic component is not seriously affected except for it becomes more sharp in the TLs ($\Delta H \simeq 30 \text{ Oe}$) when compared to the BLs ($\Delta H \simeq 50 \text{ Oe}$) as may be easily seen in Figs.5(a) and 6(a), respectively. This fact indicates that in the TLs the out-of-plane rotation is forced by the interaction of the outer NiFe layers. (iii) The SC exhibits transverse magnetization component since it interacts rigidly with the outer FM layers (see Fig.4(b)). (iv) Finally, although the out-of-plane rotation of the magnetization is surely related to the strong magnetoresistance effect that is observed in the TLs (the relative peaks of the $m_{tran}(H)$ and $V(H)$ curves presented in Figs.5(a) and 5(b), respectively clearly coincide), for the BLs it has no or minor influence (the relative peaks of the $m_{tran}(H)$ and $V(H)$ curves presented in Figs.6(a) and 6(b), respectively are clearly not related). Based on these experimental facts below we discuss the most possible mechanism for their interpretation. We discuss first the TLs where the effect is peculiar.

As stated above, reason (iv) indicates that in the TLs the magnetization's out-of-plane rotation surely contributes to the observed effect. However, we believe that in the TLs an extra ingredient should also exist that promotes the magnetoresistance effect so strongly since in the BLs the magnetization's out-of-plane rotation also occurs but the accompanied magnetoresistance effect is only minor. This extra ingredient comes from reasons (ii) and (iii): in the TLs it is an *interaction* mechanism between the outer NiFe layers that is getting involved. Since the Nb interlayer is rather thick we believe that this interaction refers rather to a stray-fields induced magnetostatic coupling of the outer NiFe layers than an exchange one. On the other hand, although in the BLs this mechanism could also be involved, it surely has a mild contribution since the single NiFe layer doesn't have the opportunity to get coupled with a second one so that the Nb interlayer is not pierced effectively by the transverse stray fields. Here we present a complete discussion on the possibility of such magnetostatic coupling.

It is well known that in relevant TLs of normal or insulating interlayer the interaction of the outer FM layers through stray fields that occur at domain walls may lead to significant magnetostatic coupling.^{17,18} This behavior is expected to be pronounced when the FM layers have a multi-domain magnetic state, that is in the low magnetic field regime, near coercivity. S. Parkin and colleagues have shown^{17,18} that such stray-fields coupling that occurs at domain walls plays a unique role in FM-IN-FM and FM-NM-FM TLs (IN and NM stand for insulator and non-magnetic metal, respectively) since it initiates potently the distinct magnetic character of even quite different outer FM layers. Accordingly, in our case the partial out-of-plane rotation of the TL's magnetization that we observe in the normal state (see Fig.4(a)), and most importantly *the unique out-of-plane rotation of the SC's magnetization that we observe in the supercon-*

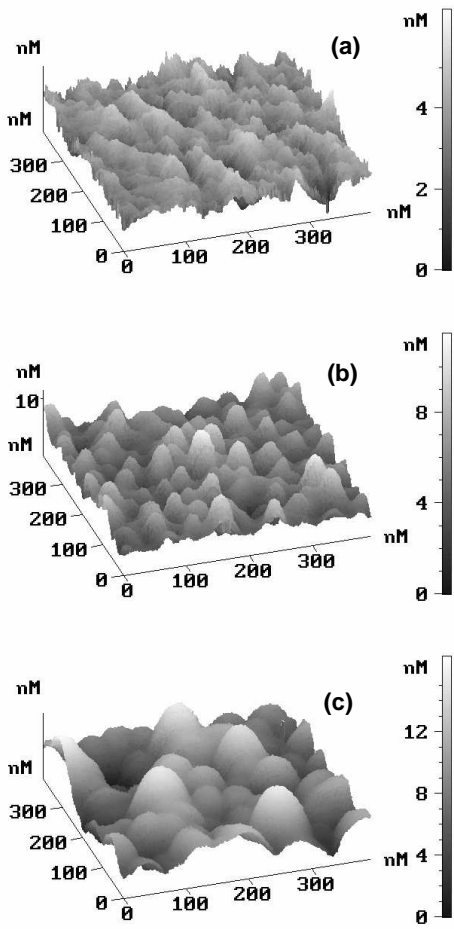


FIG. 7: Representative AFM images obtained in (a) a NiFe(19) layer, (b) a NiFe(19)-Nb(50) BL, and (c) a NiFe(19)-Nb(50)-NiFe(38) TL. In all cases the presented areas are $0.4 \times 0.4 \mu\text{m}^2$. Notice the different scales in the respective vertical black-and-white bars among panels (a)-(c).

TABLE I: Peak-to-peak, mean and root-mean-square roughness values for samples NiFe(19) SL19, NiFe(19)-Nb(50) BL and NiFe(19)-Nb(50)-NiFe(38) TL.

	peak-to-peak (nm)	mean (nm)	root-mean-square (nm)
SL19	6.3	3.2	0.7
BL	11.3	4.9	1.4
TL	16.7	8.1	2.8

ducting state (see Fig.4(b)) are probably motivated by such a stray-fields magnetostatic coupling of the outer NiFe layers: in consistency with the mechanism proposed in Refs.17,18 the out-of-plane rotation that we observe in our data occurs progressively in the low field regime where as the zeroing of the longitudinal component implies many domains get formed so that this mechanism could be activated.

The occurrence of such stray-fields coupling between the outer NiFe layers could also be promoted when sig-

nificant roughness exists at the interfaces.^{17,18,19,20} In order to investigate this possibility we performed a thorough AFM study of our samples. Representative results are shown in Figs.7(a)-7(c). Panel (a) refers to a NiFe(19) single layer (SL), panel (b) to the top surface of a NiFe(19)-Nb(50) BL, and panel (c) to the top surface of a NiFe(19)-Nb(50)-NiFe(38) TL. In all cases the presented areas are $0.4 \times 0.4 \mu\text{m}^2$. We studied all these structures because we wanted to examine if the surface roughness presents an evolution from layer to layer. Notice that the scale in the respective vertical black-and-white bars is different among panels (a)-(c). The obtained values for each sample are displayed in Table I. These data reveal that the roughness of the interfaces exhibits an evolution as a new layer is progressively added to the previous one(s). Thus, the magnetostatic coupling of the outer NiFe layers could be enhanced through local "guidance" of the stray fields by the roughness of the interfaces.^{17,18,19,20}

Ultimately, the magnetostatic coupling discussed above could motivate the magnetoresistance peaks that we observe as following: the stray fields emerge naturally near coercivity owing to the attained multidomain magnetic state so that they interconnect vis-a-vis domains that are hosted in the outer NiFe layers. Since these stray fields evolve in the whole surface of the NiFe layers they penetrate completely the Nb interlayer (see the schematic inset (c) in Fig.5). Depending on the specific characteristics of the employed FM layers (exchange field, size of magnetic domains, width and kind -Neel or Bloch- of domain walls, etc) and of the SC interlayer (lower and upper critical field values, bulk pinning force, etc) the FMs' stray fields will primarily exceed the SC's lower critical field and secondarily, in case that they are intense, even the SC's upper critical field could *locally* be exceeded, at least extremely close to its T_c^{SC} where it attains low values. These two different cases are discussed in the two following paragraphs.

Case (a): In case where only the SC's lower critical field is exceeded by the FMs' stray fields dissipation should set in due to the following reason: since the magnetostatic coupling of the outer NiFe layers leads to a transverse magnetization field that penetrates entirely the Nb interlayer we may assume that vortices enter the Nb interlayer in the form of "chains" that are mainly positioned above domain walls. Thus, the SC interlayer is in the mixed state. The current applied during our transport measurements is normal to such "chains" of vortices so that it exerts a Lorentz force on them.²⁷ This leads to movement of vortices which is well known that results in dissipation.²⁷ Eventually, as we lower the temperature the magnetoresistance peaks become progressively smaller since bulk pinning sets in and vortices are no longer free to move, or the increased lower critical field exceeds the stray fields so that a dissipationless Meissner state is ultimately recovered.²⁷ This explanation resembles the one that was presented by V.V. Ryazanov et al. in Ref.21 for Nb-Cu_{0.43}Ni_{0.57} BLs.

Case (b): In this case we may assume that since the pronounced magnetoresistance effect is observed extremely close to T_c^{SC} where except for the SC's lower critical field, its upper critical field is also very low, the FMs' stray fields could even *locally* overstep it. Thus, *localized* normal areas of the SC that lie above FM areas where intense stray fields emerge should contribute extra dissipation. Eventually, in the scenario discussed here the disappearance of the magnetoresistance peaks is owing to the fact that as we progressively lower the temperature the SC's upper critical field exceeds the stray fields that interconnects the outer FMs so that bulk superconductivity is completely restored throughout the whole SC interlayer. Of course, since the lower critical field is always smaller than the upper critical one we expect that the mechanism described in case (a) (case(b)) should have a major (minor) contribution to the observed magnetoresistance effect.

Here let us compare our results with current experiments that are very relevant to our work. Regarding the TLs, we believe that the specific characteristics of our films owing to their preparation process (soft magnetic behavior, no uniaxial magnetic anisotropy, noticeable interface roughness that evolves from layer to layer) explain the differences in both the magnitude of the magnetoresistance and the proposed mechanisms between the TLs studied in Refs.3,4 and in our work. A. Yu. Rusanov et al. reported⁴ on the magnetoresistance of similar NiFe-Nb-NiFe TLs and attributed the magnetoresistance peaks that they observed to the antiparallel alignment of the outer NiFe layers. Their samples were deposited while the substrates were directed along the sputtering chamber's residual fields so that they exhibit strong uniaxial anisotropy with the easy axis of magnetization placed along their long dimension. Thus, in their case as the magnetic field passes through zero the magnetization of each NiFe layer participating a TL reverses *coherently* and probably in-plane without exhibiting significant out-of-plane component (although data on the transverse magnetic component are not presented in Ref.4). According to the same arguments the significant difference between the magnetoresistance values observed in Ref.4 and in our work is also explained. In Ref.4 it is reported that by using the definition $(R_{max} - R_{min})/R_{nor} \times 100\%$ the maximum magnetoresistance value amounts to 5% – 10%, while in our case the respective value is 45% (see Fig.2(a)) for the TL presented in this work (in other samples we even observed values exceeding slightly 50%). Also, V. Peña et al.³ have reported on a magnetoresistance effect observed in $\text{La}_{0.7}\text{Ca}_{0.3}\text{MnO}_3$ - $\text{YBa}_2\text{Cu}_3\text{O}_7$ - $\text{La}_{0.7}\text{Ca}_{0.3}\text{MnO}_3$ TLs. By using the definition $(R_{max} - R_{min})/R_{min} \times 100\%$ the authors noted a magnetoresistance increase of 1000% in the superconducting state. Thus, quantitatively the effect that we observe (see Fig.2(a)) is identical to the one reported in Ref.3. This is quite surprising since both constituents $\text{La}_{0.7}\text{Ca}_{0.3}\text{MnO}_3$ and $\text{YBa}_2\text{Cu}_3\text{O}_7$ have very different properties from the materials used in our TLs. While

$\text{La}_{0.7}\text{Ca}_{0.3}\text{MnO}_3$ is highly spin polarized (almost 100%) NiFe has a comparatively low spin polarization (45%). Also, $\text{YBa}_2\text{Cu}_3\text{O}_7$ is a representative high- T_c material, while Nb is a well studied low- T_c one. Consequently, we may assume that the observation of a similar (if not identical) magnetoresistance effect in both $\text{Ni}_{80}\text{Fe}_{20}$ -Nb- $\text{Ni}_{80}\text{Fe}_{20}$ (Ref.4 and this work) and $\text{La}_{0.7}\text{Ca}_{0.3}\text{MnO}_3$ - $\text{YBa}_2\text{Cu}_3\text{O}_7$ - $\text{La}_{0.7}\text{Ca}_{0.3}\text{MnO}_3$ (Ref.3) TLs could imply a generic underlying mechanism that doesn't depend on specific characteristics as the spin polarization of the FM and the pairing mechanism of the SC. Examining the influence of the transverse magnetic component in all relevant TLs could shed more light on this issue. Nevertheless, the results obtained in Refs. 3,4 and in our work are attractive for the design of low-field sensor devices.

Finally, regarding the BLs a stray-fields mechanism analogous to the one existing in the TLs is surely getting involved but with much smaller intensity since the single NiFe layer doesn't have the opportunity to get coupled magnetostatically with an adjacent one. Thus, now the stray fields don't penetrate completely the Nb interlayer so that they have only a minor influence on it.

V. SUMMARY AND CONCLUSIONS

In summary, we demonstrated that TLs comprised of low spin polarized NiFe and low- T_c Nb exhibit a pronounced magnetoresistance effect: the magnetoresistance increases two orders of magnitude when the superconducting state is reached, from the normal-state value $\Delta R/R_{nor} \times 100\% = 0.6\%$ it goes up to $\Delta R/R_{nor} \times 100\% = 45\%$ ($\Delta R/R_{min} \times 100\% = 1000\%$) for temperatures below T_c^{SC} . In contrast, the BLs exhibit a minor effect: from $\Delta R/R_{nor} \times 100\% = 3\%$ in the normal state the magnetoresistance increases only to $\Delta R/R_{nor} \times 100\% = 8\%$ ($\Delta R/R_{min} \times 100\% = 70\%$).

Magnetization data referring to the evolution of the transverse component from the normal to the superconducting state are presented for the first time. Regarding the normal state these magnetization data revealed that in the same field range where the magnetoresistance peaks are observed the TL's magnetization partially rotates out-of-plane. Surprisingly, in the superconducting regime the SC's magnetization follows rigidly the outer FM layers and also exhibits a transverse component. We attribute these facts to the magnetostatic coupling of the outer NiFe layers owing to the stray fields that, near coercivity, evolve naturally in their whole surface. As a result the "magnetically pierced" SC interlayer behaves diamagnetically not in respect to the longitudinal external magnetic field but in respect to these stray fields that interconnect the outer NiFe layers.

Thus, the strong magnetoresistance effect that is observed in the TLs around coercivity is owing to the stray fields that as they penetrate entirely the Nb interlayer they exceed either only its lower or even its upper critical field. This detail can't be elucidated by our measure-

ments. However, in the general case this should depend on the specific characteristics of the employed FM and SC constituents.

Referring to the BLs although out-of-plane rotation of the single NiFe layer is observed in the magnetization measurements, the accompanying stray fields have only a modest influence on magnetoresistance since magneto-static coupling is not realized owing to the absence of a second NiFe layer.

Note added: During the review process we become aware of the article [R. Steiner and P. Ziemann, Phys. Rev. B **74**, 094504 (2006)] which deals with the same subjects. R. Steiner and P. Ziemann study hybrid TLs and BLs consisting of Co, Fe and Nb by performing transport and *longitudinal* magnetization measurements.

However, the measurements of the longitudinal magnetic component were limited in the normal state. In addition, the authors also employ micromagnetic simulations to convincingly show that in their samples the stray fields are related to the observed dissipation peaks. In our work we employ magnetization measurements of both the *longitudinal* and *transverse* magnetic components in the TLs and their building-blocks BLs to reveal the contribution of this mechanism. Our magnetization data extend in the superconducting state uncovering important information on the coupling between the outer FM layers and the SC interlayer. Obtained by different means the basic explanation proposed in [R. Steiner and P. Ziemann, Phys. Rev. B **74**, 094504 (2006)] and in our work is the same.

- * Author to whom correspondence should be addressed; electronic address: densta@ims.demokritos.gr
- ¹ J.Y. Gu, C.-Y. You, J.S. Jiang, J. Pearson, Ya.B. Bazaliy, and S.D. Bader, Phys. Rev. Lett. **89**, 267001 (2002).
 - ² I.C. Moraru, W.P. Pratt, Jr., and N.O. Birge, Phys. Rev. Lett. **96**, 037004 (2006).
 - ³ V. Pena, Z. Sefrioui, D. Arias, C. Leon, J. Santamaria, J.L. Martinez, S.G.E. te Velthuis, and A. Hoffmann, Phys. Rev. Lett. **94**, 57002 (2005).
 - ⁴ A.Yu. Rusanov, S. Habraken, and J. Aarts, Phys. Rev. B **73**, 060505(R) (2006).
 - ⁵ D. Stamopoulos, M. Pissas, V. Karanasos, D. Niarchos, and I. Panagiotopoulos, Phys. Rev. B **70**, 054512 (2004).
 - ⁶ D. Stamopoulos, N. Moutis, M. Pissas, and D. Niarchos, Phys. Rev. B **72**, 212514 (2005).
 - ⁷ D. Stamopoulos and M. Pissas, Phys. Rev. B **73**, 132502 (2006).
 - ⁸ D. Stamopoulos, Supercond. Sci. Technol. **19** 652 (2006).
 - ⁹ D. Stamopoulos, E. Manios, and M. Pissas, Phys. Rev. B **75**, 014501 (2007).
 - ¹⁰ A.F. Volkov, F.S. Bergeret, and K.B. Efetov, Phys. Rev. Lett. **90**, 117006 (2003); *ibid*, **86**, 4096 (2001); *ibid*, Phys. Rev. B **69**, 174504 (2004).
 - ¹¹ T. Lfwander, T. Champel, J. Durst, and M. Eschrig, Phys. Rev. Lett. **95**, 187003 (2005); M. Eschrig, J. Kopu, J.C. Cuevas, and G. Schön, *ibid*, **90**, 137003 (2003).
 - ¹² M.D. Allsworth, R.A. Chakalov, M.S. Colclough, P. Mikheenko, and C.M. Muirhead, Appl. Phys. Lett. **80**, 4196 (2002); P. Mikheenko, R.A. Chakalov, R. Chakalova, M.S. Colclough, and C.M. Muirhead, Physica C **408-410**, 365 (2004).
 - ¹³ M. A. Maleki and M. Zareyan, Phys. Rev. B **74**, 144512 (2006).
 - ¹⁴ A.I. Buzdin, A.V. Vedyayev, and N.V. Ryzhanova, Europhys. Lett. **48**, 686 (1999).
 - ¹⁵ L.R. Tagirov, Phys. Rev. Lett. **83**, 2058 (1999).
 - ¹⁶ S. Takahashi, H. Imamura, and S. Maekawa, Phys. Rev. Lett. **82**, 3911 (1999); S. Takahashi, T. Yamashita, H. Imamura, and S. Maekawa, J. Magn. Magn. Mater. **240**, 100 (2002).
 - ¹⁷ S. Gider, B.U. Runge, A.C. Marley, and S.S.P. Parkin, Science **281**, 797 (1998).
 - ¹⁸ L. Thomas, M.G. Samant, and S.S.P. Parkin, Phys. Rev.

- Lett. **84**, 1816 (2000).
- ¹⁹ B.D. Schrag, A. Anguelouch, S. Ingvarsson, G. Xiao, Y. Lu, P.L. Trouilloud, A. Gupta, R.A. Wanner, W.J. Gallagher, P. M. Rice, and S.S.P. Parkin, Appl. Phys. Lett. **77**, 2373 (2000).
 - ²⁰ W.F. Egelhoff, Jr., R.D. McMichael, C.L. Dennis, M.D. Stiles, A.J. Shapiro, B.B. Maranville, and C.J. Powell, Appl. Phys. Lett. **88**, 162508 (2006).
 - ²¹ V.V. Ryazanov, V.A. Oboznov, A.S. Prokofiev, and S.V. Dubonos, Pis'ma Zh. Eksp. Teor. Fiz. **77**, 43 (2003) [JETP Lett. **77**, 39 (2003)].
 - ²² D. Stamopoulos, M. Pissas, and E. Manios, Phys. Rev. B **71**, 014522 (2005).
 - ²³ D. Stamopoulos, E. Manios, M. Pissas, and D. Niarchos, Supercond. Sci. Technol. **17** L51 (2004); D. Stamopoulos, and E. Manios, *ibid*, **18** 538 (2005).
 - ²⁴ B. Dieny, J. Magn. Magn. Mater. **136**, 335 (1994).
 - ²⁵ M.N. Baibich, J.M. Broto, A. Fert, F. Nguyen Van Dau, F. Petro, P. Eitenne, G. Creuzet, A. Friederich, and J. Chazelas, Phys. Rev. Lett. **61**, 2472 (1988).
 - ²⁶ S.S.P. Parkin, N. More, and K.P. Roche, Phys. Rev. Lett. **64**, 2304 (1990).
 - ²⁷ M. Tinkham, *Introduction to Superconductivity* (McGraw-Hill, New York, 1996).